RESEARCH ARTICLE | ANTHROPOLOGY |

The age of the opening of the Ice-Free Corridor and implications for the peopling of the Americas

Jorie Clark, Anders E. Carlson, Alberto V. Reyes, +6, and Dylan H. Rood Authors Info & Affiliations

Edited by David Meltzer, Southern Methodist University, Dallas, TX; received October 8, 2021; accepted February 2, 2022

March 21, 2022 119 (14) e2118558119 https://doi.org/10.1073/pnas.2118558119

Significance

The Ice-Free Corridor (IFC) has long played a key role in hypotheses about the peopling of the Americas. Earlier assessments of its age suggested that the IFC was available for a Clovis-first migration, but subsequent developments now suggest a pre-Clovis occupation of the Americas that occurred before the opening of the IFC, thus supporting a Pacific coastal migration route instead. However, large uncertainties in existing ages from the IFC cannot preclude its availability as a route for the first migrations. Resolving this debate over migration route is important for addressing the questions of when and how the first Americans arrived. We report cosmogenic nuclide exposure ages that show that the final opening of the IFC occurred well after pre-Clovis occupation.

Abstract

The Clovis-first model for the peopling of the Americas by ~13.4 ka has long invoked the Ice-Free Corridor (IFC) between the retreating margins of the Cordilleran and Laurentide ice sheets as the migration route from Alaska and the Yukon down to the Great Plains. Evidence from archaeology and ancient genomics, however, now suggests that pre-Clovis migrations occurred by at least ~15.5 to 16.0 ka or earlier than most recent assessments of the age of IFC opening at ~14 to 15 ka, lending support to the use of a Pacific coast migration route instead. Uncertainties in ages from the IFC used in these assessments, however, allow for an earlier IFC opening which would be consistent with the availability of the IFC as a migration route by ~15.5 to 16.0 ka. Here, we use 64 cosmogenic (^{10}Be) exposure ages to closely date the age of the full opening of the IFC at 13.8 ± 0.5 ka. Our results thus clearly establish that the IFC was not available for the first peopling of the Americas after the Last Glacial Maximum, whereas extensive geochronological data from the Pacific coast support its earlier availability as a coastal migration route.

The “Ice-Free Corridor” (IFC), which developed as a contiguous ice-free area along the eastern front of the Rocky Mountains as the coalescent margins of the late-Pleistocene Cordilleran and Laurentide Ice Sheets separated and retreated (Fig. 1), has long played a central role in hypotheses about the peopling of the Americas (1–3). Upham (4) first proposed the existence of an IFC during the last glaciation, while Johnston (5) first proposed its use as a travel route from Beringia down to the Great Plains. The subsequent discovery of the Clovis cultural complex, which is dated as early as ~13,400 calibrated ^{14}C years ago (~13.40 cal ka BP) (6, 7), was considered to be the oldest archaeological horizon in North America, forming the basis for the “Clovis-first” model for the migration south of the ice sheets that occurred by way of the IFC. At the same time, initial ^{14}C ages from the IFC supported its availability as a migration route for Clovis people (8–10).

Fig. 1.

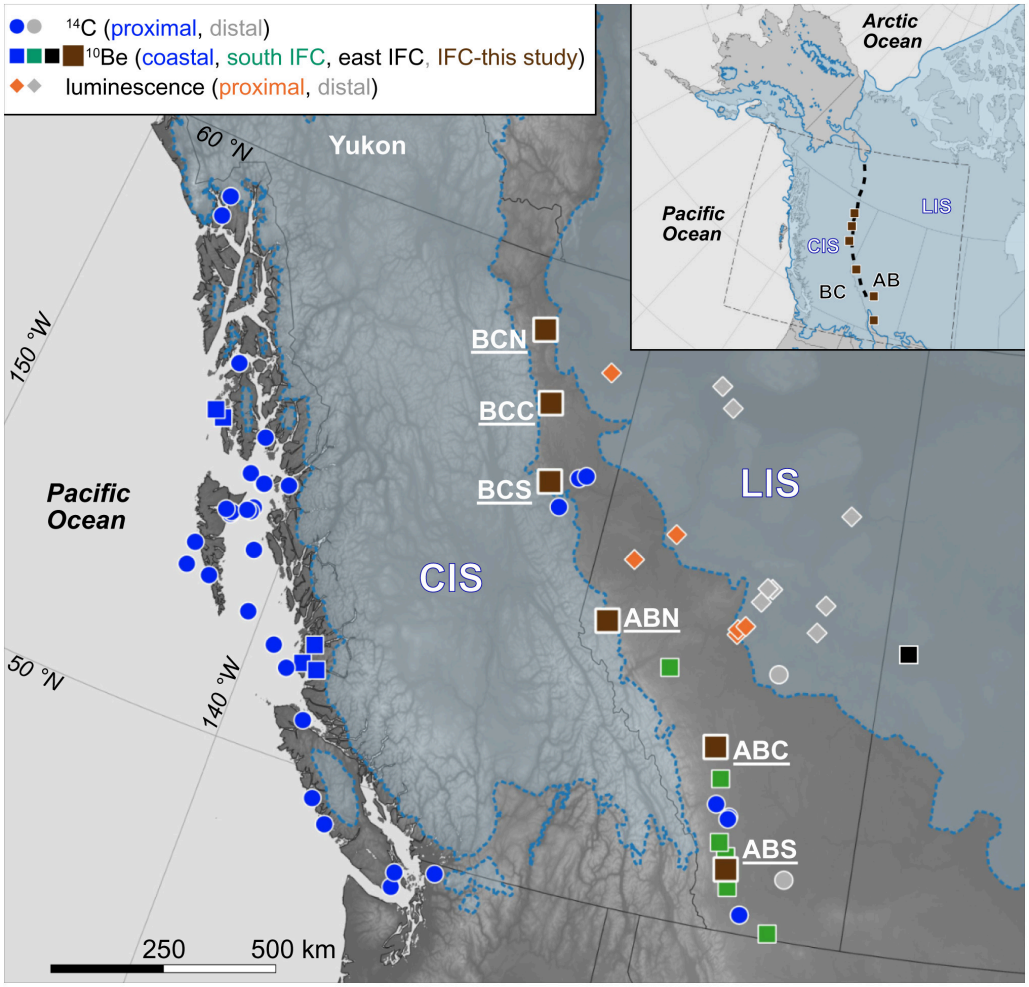

Map showing the extent of Cordilleran and Laurentide Ice Sheets after initial opening of IFC and location of dated sites. Margins of Cordilleran (CIS) and Laurentide (LIS) ice sheets at 14.2 cal ka are from ref. 55 and locations of sites with ages are discussed in Results. Sites with ^{14}C ages are shown as blue and gray circles, with the former sites occurring more proximal to ice-margin retreat and opening of initial IFC or coastal corridor, and latter sites occurring more distal to initial IFC. Sites with luminescence ages are shown as orange and gray diamonds, with the former sites occurring more proximal to ice-margin retreat and opening of the IFC, and latter sites occurring more distal to the initial IFC. Sites with ^{10}Be ages are shown as squares, with published ages are shown as blue squares constraining retreat of western Cordilleran Ice-Sheet margin (53, 54), green squares constraining opening of southern IFC (34), the black square constraining the age of deglaciation ~500 km east of the IFC (41), and brown squares (with underlined text indicating site name) representing our mean ages that constrain the opening of the IFC. Inset map shows our sample locations within the context of the approximate location of the suture zone (thick dashed line) of the CIS and LIS at the LGM ~21 ka. AB = Alberta, BC = British Columbia.

Several subsequent developments, however, have challenged the Clovis-first model as well as the

evidence for pre-Clovis occupation of the Americas south of the ice sheets by at least 15.5 to 16.0 ka (e.g., based on ages of ~15.6 cal ka BP from the Cooper's Ferry site [Idaho] (14) and estimates from genomic evidence of ~15.7 ka [95% CI 17.5 to 14.6 ka] (19)). At the same time, assessments of newer age constraints have concluded that the IFC did not open until 14 to 15 ka (19–24). Moreover, ancient genomic and radiocarbon evidence indicate that the corridor only became suitable for human travel and subsistence (i.e., biologically viable) by ~13.2 ka or earlier (25, 26), with other studies proposing even later IFC viability after ~12.6 ka (27). These developments have lent support to a proposed migration route for pre-Clovis people from Beringia down the western Canadian coast (the "coastal corridor") that largely bypassed the ice sheets (28–30). While some have suggested that the IFC route should not yet be rejected until the archaeological record supports the coastal corridor route (21, 31, 32), we note that no compelling archaeological evidence has yet been found to support a first migration through the IFC.

Despite broad agreement that the IFC was not unglaciated along its full length until 14 to 15 ka (19–24), existing ages used to support this time window are largely based on dating methods, many with large uncertainties, that include some lag between the time of deglaciation and the formation of the dated record (i.e., minimum-limiting ages) (26, 33). As we discuss further below, these same data can thus be used to argue for an earlier opening of the IFC that was available as a first-migration pathway. Similarly, arguments regarding the viability of the IFC to support first migrations are also based on dated organics that provide only minimum-limiting ages for biological productivity (25, 27). Uncertainties in existing data thus suggest that the IFC cannot yet be excluded as a potential route for pre-Clovis occupation. Resolving this debate over migration route is important for addressing the questions of when and how the first Americans arrived in regions south of the continental ice sheets.

To narrow these uncertainties in the current understanding of the age of the IFC opening, we first assess a compilation of ages that are commonly cited (in part or in entirety) to support the 14- to 15-ka time window for the age of the IFC opening (Figs. 1 and 2) (26). We then use 64 ^{10}Be surface exposure ages from 6 locations spanning ~1,200 km of the Cordilleran–Laurentide suture zone that separated to produce the IFC (Fig. 1) to directly date the opening of the IFC with sufficient precision to establish whether it was available for the first peopling of the Americas south of the ice sheets.

Fig. 2.

Compilation of ages used to constrain the timing of the opening of the IFC. Sites with ^{14}C ages are shown as blue and gray circles (2σ uncertainty), with the former sites occurring more proximal to Cordilleran–Laurentide ice-sheet suture zone and latter sites occurring more distal to ice-sheet suture zone (26) (SI Appendix, Table S2). Sites with luminescence ages are shown as orange and gray diamonds (1σ uncertainty), with the former sites occurring more proximal to Cordilleran–Laurentide ice-sheet suture zone and latter sites occurring more distal to ice-sheet suture zone (26) (SI Appendix, Table S3). Sites with ^{10}Be ages are shown as squares (1σ uncertainty), with published ages as green squares constraining opening of southern IFC (34) (SI Appendix, Table S4), gray (individual ages) and black (mean age) squares constraining the age of deglaciation ~500 km east of the IFC (41), and our ages as brown squares (with corresponding site location names ABS-BCN) constraining opening of the IFC (SI Appendix, Table S1).

Results

Previous Dating of the IFC.

Existing ages used to constrain the age of IFC opening include calibrated ^{14}C ages that have been previously screened in order to remove those known to be potentially commonly contaminated and thus result in spurious results (e.g., bulk sediments, terrestrial shells) (26) (*SI Appendix*, Table S2), a compilation of luminescence ages on sand dunes from Alberta (33) (*SI Appendix*, Table S3), and cosmogenic nuclide (^{10}Be) exposure ages on erratics from the southern section of the Cordilleran–Laurentide suture zone (34) (*SI Appendix*, Table S4). We exclude four ^{10}Be ages from this latter study in our analysis here because they are from sites immediately adjacent to two of our sampling sites, and so we instead include them with our new ^{10}Be ages from those sites. We assess all ages according to their proximity to the Cordilleran–Laurentide suture zone (Fig. 1), with the expectation that they should become younger with increasing lateral distance from the ice-sheet suture zone.

^{14}C ages typically provide only minimum-limiting ages on ice-margin retreat, owing to the unknown amount of time that lapsed between deglaciation and accumulation of reliably datable organic material

dates from 2 sites that are 200 to 400 km east of the suture zone are also ≤13.5 cal ka BP and show no longitudinal trend. Only one date is >13.5 cal ka BP (AA43652) and has been used to support the opening of the IFC by 15.0 ± 0.2 cal ka BP (32). This date, however, was measured on a standard collagen extraction from taiga vole bones that were redeposited by a low-energy mud flow. Another age on vole bones from the same unit are stratigraphically below but ∼1,600 y younger than the age 15.0 ± 0.2 cal ka BP. ^{14}C ages on organics above and below the bone-bearing unit suggest the debris flow occurred during the middle Holocene (37). Given the potential for contamination of the collagen from old carbonate as well as the lack of stratigraphic integrity and provenance of the bones, this age provides a poor constraint on IFC opening (26). However, given their minimum-limiting nature, the remaining 48 dates do not preclude the opening of the IFC well before 13.5 cal ka BP. For example, other studies of Laurentide Ice-Sheet retreat that combined ^{10}Be ages with minimum-limiting ^{14}C ages found millennial-scale lags between the timing of ice retreat and the oldest ^{14}C-dated material (36, 38, 39).

Luminescence ages on sand dunes in Alberta have been central to recent assessments of the age of the IFC (24, 26, 31–33), but these are even more problematic than the redeposited vole bone fragments. For example, the sampled sites cover a broad region of Alberta that extends from ∼150 km to 1,000 km east of the ice-sheet suture zone (Fig. 1), thus only providing minimum-limiting ages on the initial opening of the IFC. The fact that sediment sources for the sand dunes were largely derived from glacial lake sediments that became exposed following lake drainage (33) further limits their ability to date the initial opening of the IFC. Fig. 2 shows that ages from within relatively small regions can span 3.5 to 4.5 ky and that uncertainties on individual luminescence dates are high (mean ± 1 SE uncertainty is ±1.1 ky for 46 luminescence ages in ref. 33). In many cases, ages that are more proximal to the suture zone are younger than, or similar to, ages that are more distal, equivalent to a stratigraphic age reversal. Assuming full bleaching, the oldest luminescence age from the IFC zone should provide the closest constraint on ice-margin retreat. This would place the IFC as open before 15.3 ± 1.3 ka for the optically stimulated luminescence method (33) or 15.7 ± 1.6 ka for the infrared stimulated luminescence method (40).

The mean of ^{10}Be exposure ages on erratics from sites extending between 49.1°N and 53.4°N has been used to argue that the southern sector of the IFC had opened by 14.9 ± 0.9 ka (14, 22, 24, 34). However, because these sites are spaced 10s to more than 200 km apart (Fig. 1), the ages of these erratics should not be averaged together to determine the millennial- to centennial-scale timing of the ice-margin retreat. We recalculated these ages following the same protocols as for our ^{10}Be ages (*Methods*). Of the 11 dates considered here (excluding the 4 ages we combine with our ^{10}Be ages [*SI Appendix*, Table S1] and another age identified as a clear outlier because of its Holocene age), 5 sites have only one ^{10}Be age and another three sites have only two ^{10}Be ages, making outlier identification for each site difficult. If considered to contain no geologic scatter, these isolated ^{10}Be ages would place IFC opening at 18.0 ± 0.8 ka (n = 1) at ∼49.1°N, 15.5 ± 0.9 ka (n = 2) at ∼50.3°N, and 17.6 ± 0.9 ka (n = 1) at 53.4°N; the remaining 8 ages fall within this range. While the ∼17.6-ka age appears to be out of stratigraphic order, one cannot exclude this age due to ^{10}Be inheritance without a larger number of samples from the same site.

The mean of six ^{10}Be ages from closely spaced samples was used to infer the formation of the IFC after 13.5 ± 0.8 ka (41). These samples, however, are ∼500 km east of the suture zone (Fig. 1), and their ages thus only suggest that the IFC opened before 13.5 ± 0.8 ka.

Cosmogenic Exposure Ages from the IFC.

To directly date the opening of the IFC with century-scale precision, we collected multiple samples for ^{10}Be surface exposure dating from each of six sites (*SI Appendix*, Figs. S1 and S2) along a 1,200-km-long, south–north transect (∼50 to 59°N) where mapping identified the confluence of the Cordilleran and Laurentide Ice Sheets (42–44) (Fig. 1). These ages date the onset of ice-free conditions in association with ice-sheet

were exhumed from moraine degradation, we sampled glacially transported boulders resting on bedrock and, at site British Columbia north (BCN), glacially eroded bedrock (Fig. 3). Five of the sites are on topographic highs above the elevations of former proglacial lakes (45), and there is no evidence of lake cover at the one site on the plains of west–central Alberta (ABC) (34, 43). We collected >10 samples at 5 of the sites and 5 samples from a 6 site (British Columbia central [BCC]) to assess geologic scatter. Given their proximity to our two southernmost sites (Alberta south [ABS], ABC), we also include four ^{10}Be ages from ref. 34. (Fig. 1 and *SI Appendix*, Fig. S1 and Table S1).

Fig. 3.

Photographs of representative glacial erratics sampled for cosmogenic ^{10}Be dating. (A) Sample ABC-5-16. (B) Sample ABS-1-16.

We calculated individual ^{10}Be ages using the Arctic production rate (46) and Lal/Stone time-varying scaling (47). We use the Arctic production rate calibration data set (46) for our high-latitude sites as opposed to the global production rate dataset (47) because it better accounts for the regional variability of the cosmic ray flux and associated production rate. We note, however, that the exposure ages calculated using the global production rate calibration data set are, on average, only 4% younger than our preferred exposure ages, which is within the 1σ external uncertainties.

We made no snow cover, vegetation, or erosion corrections. Given the major climate shifts of the last

the tops of boulders, where snow cover is more likely to blow off by wind; and we find excellent agreement between boulders and bedrock samples at site BCN where the former should have a lesser impact from snow cover than the latter. Vegetation similarly changed over the last 14,000 y, but as with snow cover, it has a low density and thus low shielding of cosmic rays. We sampled boulder surfaces that showed little-to-no erosion, but typical erosion rates (<1 mm ka^{-1}) suggest that erosion is not an issue at these timescales (48). We accounted for changes in sample elevation from isostatic uplift by using an iterative approach with isostatic rebound models (49) and ice-sheet simulations (50). After removing outliers based on the constraints that samples cannot date from older than the Last Glacial Maximum (LGM; 26.5 to 19 ka) or be from the Holocene (<11.7 ka), we calculated the timing and uncertainty of deglaciation at each site using the arithmetic mean and SE (Fig. 2 and *SI Appendix*, Table S1 and Fig. S4), with the latter also including production rate uncertainty and reported as the external uncertainty to facilitate comparison with other dating methods for IFC opening.

Our ^{10}Be ages suggest that the IFC opened first at 15.4 ± 0.7 ka at our southernmost site (ABS, 50.0°N, n = 9). The IFC then progressively opened from the north and the south, with our mean age of 14.8 ± 0.7 ka at site ABC (52.2°N, n = 10) being (within uncertainty) the same as ^{10}Be ages from our two northern sites that suggest the northern section of the IFC began to open (14.4 ± 0.6 ka, BCN, 58.7°N, n = 10; 14.5 ± 0.7 ka, BCC, 56.1°N, n = 4) (Fig. 2). The center of the IFC then opened at 14.2 ± 0.6 ka at site Alberta north (ABN) (53.9°N, n = 11) and lastly at 13.8 ± 0.5 ka at site British Columbia south (BCS) (56.1°N) (Fig. 2), with the latter mean age being particularly robust as it is based on 15 ^{10}Be ages with no outliers. Indeed, the SE at this site is only ±0.1 ka (±0.7%), with the remaining ±0.4 ka coming from the production rate uncertainty of ±3.8% (46). A Monte Carlo experiment using the distribution of ^{10}Be exposure ages from the BCS site suggests that ~>50 exposure ages are required to drive the site SE below ±0.1 ky (*SI Appendix*, Fig. S4), indicating that our analyses for this site are at the practical limit of precision for this direct dating technique and the ±0.5-ka external uncertainty cannot be realistically improved upon without reduction in production rate uncertainty. Finally, we note that site BCS (56.1°N, 122.2°W) is located just west of two sites (Charlie Lake, 56.3°N, 120.9°W; Spring Lake, 55.5°N, 119.6°W) where evidence of steppe vegetation and a variety of animals first appears at ~12.6 ka (27), suggesting that the final opening of the IFC occurred ~1.2 ky before this area became biologically viable.

Fig. 2 compares our ^{10}Be ages with the existing chronology for the IFC assessed above. Except for the calibrated ^{14}C age on the taiga vole bones (AA43652), all calibrated ^{14}C ages are younger than the mean ^{10}Be ages, consistent with the ^{14}C ages being minimum-limiting ages on deglaciation. At the same time, the calibrated ^{14}C age on taiga vole bones is ~1 ky older than the mean ^{10}Be age of 13.8 ± 0.5 ka from the nearby BCS site and ~2.2 ky older than nearby sites recording the first colonization of the area by plants and animals (27), which is consistent with the bones being contaminated by old carbonate (26). Many luminescence ages that are proximal to, but still east of, the central IFC area are older than the mean ^{10}Be ages for deglaciation from these latitudes, further identifying age reversals that are possibly due to mixing with incompletely bleached glaciofluvial or glaciolacustrine sand prior to burial. Published ^{10}Be ages from the southern IFC include two that are significantly older than our mean ages and one (8.6 ± 0.3 ka) that is significantly younger (34). The remaining ages are similar to our mean ages, but again cannot be combined as a single population to calculate a mean age because of the large distances between the sites. Of the two published ages included with our ABS ages, one is an outlier (181 ± 4 ka) and the other (15.8 ± 0.5 ka) is similar to the mean age (15.4 ± 0.7 ka). Of the two published ages included with our ABC ages, one is also an outlier (24.2 ± 0.9 ka), whereas the other age (16.4 ± 0.6 ka) is significantly older than the mean age (14.8 ± 0.7 ka), providing an example of how a single age affected by geologic scatter can provide an inaccurate age for IFC opening. Finally, the ^{10}Be ages from the Beaver River site in west–central Saskatchewan ~500 km east of the suture zone (mean age of 13.5 ± 0.8 ka) (41) are consistent with the ~13.8-ka timing for opening of the IFC from our 15 ^{10}Be ages at site BCS.

Discussion

Our ^{10}Be chronology closely dates the final opening of the IFC as occurring at 13.8 ± 0.5 ka (Fig. 4*A*), establishing that the IFC was not available as a migration route for the peopling of the Americas that had occurred before ∼15.6 ka suggested by current archaeological and ancient genomic evidence (Fig. 4*B*). In contrast, multiple ^{14}C and ^{10}Be ages (51–55) from the coastal corridor (*SI Appendix*, Tables S5 and S6) indicate that retreat of the western margin of the Cordilleran Ice Sheet and associated postglacial uplift occurred early enough to have provided a migration route for people prior to the earliest known archaeological sites south of the ice sheets (Fig. 4*A*). We note that these first peoples would likely still have faced considerable difficulties in navigating the largely glaciated coastline (51). Further dating of western CIS margin retreat and relative sea level change will improve our understanding of the paleogeography of this coastal corridor, which can then serve as a guide in the search for the archaeological evidence that is required to confirm this coastal migration route.

Fig. 4.

Age constraints on opening of IFC, coastal corridor, and first peopling of the Americas south of the ice sheets. (A) Sites with ^{14}C (2σ uncertainty) and ^{10}Be (1σ uncertainty) ages constraining retreat of western margin of the Cordilleran Ice Sheet and emergence of ice-free areas are shown as blue horizontal lines and squares, respectively (52–55) (SI Appendix, Tables S5 and S6). Sites with ^{10}Be ages constraining opening of the IFC are shown as brown squares (1σ uncertainty) (this study). (B) Age constraints from ancient genomics (19) and archaeological sites for first peopling of the Americas south of the ice sheets. Ages from archaeological sites (SI Appendix, Table S7) are labeled as Paisley Caves, OR (PC) (12); the Page-Ladson site, FL (PL) (15); the Debra L. Friedkin site, TX (DF) (16); and the Cooper's Ferry site, ID (CF) (14).

Methods

Field Sampling.

We collected multiple samples for ^{10}Be surface exposure dating from each of six sites located along a 1,200-km-long south–north transect (~50 to 59°N) (*SI Appendix*, Figs. S1 and S2) where mapping identifies the confluence of the Cordilleran and Laurentide Ice Sheets (42, 43, 56) (Fig. 1). The ^{10}Be ages at each site date the onset of ice-free conditions from ice-sheet separation and thus the initial opening of the IFC at that location. This contrasts with existing geochronological data used to constrain the age of IFC opening which only minimum-limiting ages on ice-margin retreat since they record some unknown amount of time between deglaciation and accumulation of reliably datable material as well as the fact that many dated sites extend from ~150 km to 1,000 km east of the ice-sheet suture zone.

Samples for ^{10}Be surface exposure ages from boulders on bedrock were collected at five sites (ABS, ABC, ABN, BCS, BCC) with a sixth site (BCN) consisting of a mixture of boulder-on-bedrock samples (n = 4) and glacier-scoured bedrock samples (n = 6). Sampling followed prior methods used to document ice-sheet-scale changes in ice margins and area of the IFC (4, 5, 38, 57). Each of these sites is located near the mapped confluence of the Cordilleran–Laurentide Ice Sheets (Fig. 1) and was chosen for its simple deglacial history, with the exposure of the boulder surface being due to separation of the two ice sheets with no potential cover by proglacial lakes.

ABS is the southernmost site (50.1°N, 113.8°W, ~1,200 m above modern sea level); we collected 10 samples from this sample site and include 2 additional ages from ref. 34. (ALT-MM-15-08, ALT-MM-15-09) (*SI Appendix*, Fig. S1). All boulders are quartzite except ABS-10-16 which is granitic. At the ABC site (52.2°N, 114.8°W, ~1,100 m above modern sea level), we collected samples from 12 quartzite boulders and combined them with 2 ages from ref. 34. (ALT-MM-15-14, ALT-MM-15-15) (*SI Appendix*, Fig. S1). ABN (54.0°N, 119.0°W, ~1,800 m above modern sea level) consists of 12 quartz-rich sandstone boulders (*SI Appendix*, Fig. S1). At BCS (56.1°N, 122.2°W, ~1,100 m above modern sea level), we sampled 15 sandstone boulders resting on bedrock (*SI Appendix*, Fig. S2), while we found only 5 samples for collection at BCC (57.5°N, 122.9°W, ~1,200 m above modern sea level) (*SI Appendix*, Fig. S2). For BCN (58.7°N, 123.8°W, ~1,000 m above modern sea level), we sampled only 4 sandstone boulders (BCN-4-16, BCN-5-16, BCN-7-16, BCN-8-16), which we supplemented with an additional 6 sandstone bedrock samples to give a total of 10 samples (*SI Appendix*, Fig. S2).

^{10}Be Target Preparation and Measurement.

Thirty-four samples were prepared at PRIME Laboratory at Purdue University (6 = ABS, 8 = ABC, 5 = ABN, 5 = BCS, 5 = BCC, 5 = BCN) following standard techniques (www.physics.purdue.edu/primelab/) with another 30 samples prepared at CosmIC Laboratories at Imperial College London (4 = ABS, 4 = ABC, 7 = ABN, 10 = BCS, 0 = BCC, 5 = BCN) using standard procedures (8). ^{10}Be concentrations and uncertainties are provided in *SI Appendix*, Table S1.

Age Calculation and Isostatic Rebound.

We calculated ^{10}Be ages using the Lal/Stone time-varying scaling (47) and the Arctic ^{10}Be production rate (46). Use of another scaling (LSD; 58) does not change our results or conclusions. We do not correct for changes in atmospheric pressure as this has been shown to have a negligible impact on the production rate once the total time since deglaciation is considered (38, 57). Because the Cordilleran–Laurentide Ice-Sheet suture zone has undergone extensive isostatic rebound following deglaciation (49, 50), we estimate the impact of rebound on the surface exposure ages and correct for this influence on the final age (59). This is accomplished using ice-sheet model simulations following ref. 50.

We calculated average deglacial ages for each site following the methods of refs. 38 and 57 and include the four additional ^{10}Be ages from ref. 34 that are adjacent to ABS and ABC (*SI Appendix*, Fig. S3). Outliers that are either at least as old as the LGM (>19 ka) or Holocene (<11.7 ka) in age were identified and excluded, which excluded - samples from the 68 samples, 2 of which are from ref. 34. ABS contained three pre-LGM outliers while ABC had four LGM-age outliers (*SI Appendix*, Fig. S3). One sample at ABN and another at BCC were identified as Holocene-age outliers (*SI Appendix*, Fig. S3). Following exclusion of these nine outlier samples, we determined the arithmetic mean and SE for each site, which produced the largest uncertainty in the mean, making this a conservative approach (38). We then added the ^{10}Be production rate uncertainty of ±3.8% to the SE in quadrature to determine the external uncertainty of the mean for the timing of deglaciation and the opening of the IFC.

Data Availability

All study data are included in the article and/or *SI Appendix*.

Acknowledgments

H. Bervid aided in the fieldwork. J. M. Young and S. L. Norris shared a compilation of location data for previously published localities related to the IFC. We greatly appreciate the comments by David Meltzer and two reviewers that led to an improved paper. This work was supported by NSF Award EAR-1552230 (J.C. and A.E.C.), Natural Sciences and Engineering Research Council of Canada Discovery Grants (A.V.R., G.A.M., and L.T.), and the Australian Nuclear Science Technology Organization (ANSTO) Research Portal Proposal AP12612 (D.H.R.).

Supporting Information

Appendix 01 (PDF)

DOWNLOAD | 801.86 KB

References

1 E. Antevs, The spread of aboriginal man to North America. *Geogr. Rev.* **25**, 302–309 (1935).
Crossref | Google Scholar

2 C. V. Haynes Jr., Fluted projectile points: Their age and dispersion: Stratigraphically controlled radiocarbon dating provides new evidence on peopling of the New World. *Science* **145**, 1408–1413 (1964).
Crossref | PubMed | Google Scholar

3 P. S. Martin, The discovery of America: The first Americans may have swept the Western Hemisphere and decimated its fauna within 1000 years. *Science* **179**, 969–974 (1973).
Crossref | PubMed | Google Scholar

4 W. Upham, *The Glacial Lake Agassiz* (U.S. Geological Survey, Washington, D.C., 1895), pp. 1–658.
Google Scholar

5 W. A. Johnston, "Quaternary geology of North America in relation to the migration of man" in *The American Aborigines*, T. Origin, D. J. Antiquity, Eds. (University of Toronto Press, Toronto, Canada, 1933), pp. 9–45.

6 M. R. Waters, T. W. Stafford, D. L. Carlson, The age of Clovis-13,050 to 12,750 cal yr BP. *Sci. Adv.* **6**, eaaz0455 (2020).

Crossref | PubMed | Google Scholar

7 D. S. Miller, V. T. Holliday, J. Bright, "Clovis across the continent" in *Paleoamerican Odyssey*, K. E. Graf, C. V. Ketron, M. R. Waters, Eds. (Texas A&M Univ. Press, College Station, TX, 2014), pp. 207–220.

Google Scholar

8 B. O. K. Reeves, The nature and age of the contact between the Laurentide and Cordilleran ice sheets in the western interior of North America. *Arct. Alp. Res.* **5**, 1–16 (1973).

Crossref | Google Scholar

9 J. M. White, R. W. Mathewes, W. H. Mathews, Radiocarbon dates from Boone Lake and their relation to the ice-free corridor in the Peace River District of Alberta, Canada. *Can. J. Earth Sci.* **16**, 1870–1874 (1979).

Crossref | Google Scholar

10 R. J. Mott, L. E. Jackson, An 18000-year palynological record from the southern Alberta segment of the classical Wisconsinan ice-free corridor. *Can. J. Earth Sci.* **19**, 504–513 (1982).

Crossref | Google Scholar

11 T. D. Dillehay et al., Monte Verde: Seaweed, food, medicine, and the peopling of South America. *Science* **320**, 784–786 (2008).

Crossref | PubMed | Google Scholar

12 M. T. P. Gilbert et al., DNA from pre-Clovis human coprolites in Oregon, North America. *Science* **320**, 786–789 (2008).

Crossref | PubMed | Google Scholar

13 D. L. Jenkins et al., Clovis age Western Stemmed projectile points and human coprolites at the Paisley Caves. *Science* **337**, 223–228 (2012).

Crossref | PubMed | Google Scholar

14 L. G. Davis et al., Late upper paleolithic occupation at Cooper's Ferry, Idaho, USA, similar to 16,000 years ago. *Science* **365**, 891–897 (2019).

Crossref | PubMed | Google Scholar

15 J. J. Halligan et al., Pre-Clovis occupation 14,550 years ago at the Page-Ladson site, Florida, and the peopling of the Americas. *Sci. Adv.* **2**, e1600375 (2016).

Crossref | PubMed | Google Scholar

16 M. R. Waters et al., Pre-Clovis projectile points at the Debra L. Friedkin site, Texas-implications for the Late Pleistocene peopling of the Americas. *Sci. Adv.* **4**, eaat4505 (2018).

Crossref | PubMed | Google Scholar

17 B. Llamas et al., Ancient mitochondrial DNA provides high-resolution time scale of the peopling of the Americas. *Sci. Adv.* **2**, e1501385 (2016).

Crossref | PubMed | Google Scholar

18 J. V. Moreno-Mayar et al., Terminal Pleistocene Alaskan genome reveals first founding population of Native Americans. *Nature* **553**, 203–207 (2018).

Crossref | PubMed | Google Scholar

19 E. Willerslev, D. J. Meltzer, Peopling of the Americas as inferred from ancient genomics. *Nature* **594**, 356–364 (2021).

Crossref | PubMed | Google Scholar

20 T. J. Braje, T. C. Rick, T. D. Dillehay, J. M. Erlandson, R. G. Klein, Arrival routes of first Americans uncertain-response. *Science* **359**, 1225 (2018).

Crossref | PubMed | Google Scholar

21 B. A. Potter et al., Arrival routes of first Americans uncertain. *Science* **359**, 1224–1225 (2018).

Crossref | PubMed | Google Scholar

22 M. R. Waters, Late Pleistocene exploration and settlement of the Americas by modern humans. *Science* **365**, eaat5447 (2019).

Crossref | PubMed | Google Scholar

23 L. G. Davis, D. B. Madsen, The coastal migration theory: Formulation and testable hypotheses. *Quat. Sci. Rev.* **249**, 106605 (2020).

Crossref | Google Scholar

24 T. J. Braje et al., Fladmark+40: What have we learned about a potential Pacific Coast peopling of the Americas? *Am. Antiq.* **85**, 1–21 (2020).

Crossref | Google Scholar

25 P. D. Heintzman et al., Bison phylogeography constrains dispersal and viability of the Ice Free Corridor in western Canada. *Proc. Natl. Acad. Sci. U.S.A.* **113**, 8057–8063 (2016).

Crossref | PubMed | Google Scholar

26 D. Froese, J. M. Young, S. L. Norris, M. Margold, Availability and viability of the ice-free corridor and Pacific coast routes for the peopling of the Americas. *SAA Archaeol. Rec.* **19**, 27–33 (2019).

Google Scholar

27 M. W. Pedersen et al., Postglacial viability and colonization in North America's ice-free corridor. *Nature* **537**, 45–49 (2016).

Crossref | PubMed | Google Scholar

28 K. R. Fladmark, Routes: Alternate migration corridors for Early Man in North America. *Am. Antiq.* **44**, 55–69 (1979).

Crossref | Google Scholar

29 C. A. S. Mandryk, H. Josenhans, D. W. Fedje, R. W. Mathewes, Late Quaternary paleoenvironments of Northwestern North America: Implications for inland versus coastal migration routes. *Quat. Sci. Rev.* **20**, 301–314 (2001).

Crossref | Google Scholar

Crossref | Google Scholar

31 B. A. Potter et al., Early colonization of Beringia and Northern North America: Chronology, routes, and adaptive strategies. *Quat. Int.* **444**, 36–55 (2017).

Crossref | Google Scholar

32 B. A. Potter et al., Current evidence allows multiple models for the peopling of the Americas. *Sci. Adv.* **4**, eaat5473 (2018).

Crossref | PubMed | Google Scholar

33 K. Munyikwa, T. M. Rittenour, J. K. Feathers, Temporal constraints for the Late Wisconsinan deglaciation of western Canada using eolian dune luminescence chronologies from Alberta. *Palaeogeogr. Palaeoclimatol. Palaeoecol.* **470**, 147–165 (2017).

Crossref | Google Scholar

34 M. Margold et al., Beryllium-10 dating of the Foothills Erratics Train in Alberta, Canada, indicates detachment of the Laurentide Ice Sheet from the Rocky Mountains at similar to 15 ka. *Quat. Res.* **92**, 469–482 (2019).

Crossref | Google Scholar

35 H. E. Wright, Surge moraines of the Klutlan Glacier, Yukon Territory, Canada—Origin, wastage, vegetation succession, lake developmen, and application to the late-glacial of Minnesota. *Quat. Res.* **14**, 2–18 (1980).

Crossref | Google Scholar

36 T. V. Lowell et al., Near-constant retreat rate of a terrestrial margin of the Laurentide Ice Sheet during the last deglaciation. *Geology* **49**, 1511–1515 (2021).

Crossref | Google Scholar

37 R. J. Hebda, J. A. Burns, M. Geertsema, A. J. T. Jull, AMS-dated late Pleistocene taiga vole (Rodentia: *Microtus xanthognathus*) from northeast British Columbia, Canada: A cautionary lesson in chronology. *Can. J. Earth Sci.* **45**, 611–618 (2008).

Crossref | Google Scholar

38 D. J. Ullman et al., Final Laurentide ice-sheet deglaciation and Holocene climate-sea level change. *Quat. Sci. Rev.* **152**, 49–59 (2016).

Crossref | Google Scholar

39 D. J. Leydet et al., Opening of glacial Lake Agassiz's eastern outlets by the start of the Younger Dryas cold period. *Geology* **46**, 155–158 (2018).

Crossref | Google Scholar

40 S. A. Wolfe, D. J. Huntley, J. Ollerhead, Relict Late Wisconsinan dune fields of the Northern Great Plains, Canada. *Géogr. Phys. Quat.* **58**, 323–336 (2004).

Google Scholar

41 S. L. Norris et al., Rapid retreat of the southwestern Laurentide Ice Sheet during the Bølling-Allerød interval. *Geology*, https://doi.org/10.1130/G49493.1 (2022).

Google Scholar

Quat. Int. **32**, 21–32 (1996).

Crossref | Google Scholar

43 L. E. Jackson, F. M. Phillips, K. Shimamura, E. C. Little, Cosmogenic Cl-36 dating of the Foothills erratics train, Alberta, Canada. *Geology* **25**, 195–198 (1997).

Crossref | Google Scholar

44 G. M. D. Hartman, J. J. Clague, R. W. Barendregt, A. V. Reyes, Late Wisconsinan Cordilleran and Laurentide glaciation of the Peace River Valley east of the Rocky Mountains, British Columbia. *Can. J. Earth Sci.* **55**, 1324–1338 (2018).

Crossref | Google Scholar

45 D. S. Lemmen, A. Duk-Rodkin, J. M. Bednarski, Late glacial drainage systems along the northwestern margin of the Laurentide Ice Sheet. *Quat. Sci. Rev.* **13**, 805–828 (1994).

Crossref | Google Scholar

46 N. E. Young, J. M. Schaefer, J. P. Briner, B. M. Goehring, A Be-10 production-rate calibration for the Arctic. *J. Quat. Sci.* **28**, 515–526 (2013).

Crossref | Google Scholar

47 G. Balco, J. O. Stone, N. A. Lifton, T. J. Dunai, A complete and easily accessible means of calculating surface exposure ages or erosion rates from Be-10 and Al-26 measurements. *Quat. Geochronol.* **3**, 174–195 (2008).

Crossref | Google Scholar

48 G. Balco, Contributions and unrealized potential contributions of cosmogenic-nuclide exposure dating to glacier chronology, 1990–2010. *Quat. Sci. Rev.* **30**, 3–27 (2011).

Crossref | Google Scholar

49 K. Lambeck, A. Purcell, S. Zhao, The North American Late Wisconsin ice sheet and mantle viscosity from glacial rebound analyses. *Quat. Sci. Rev.* **158**, 172–210 (2017).

Crossref | Google Scholar

50 L. Tarasov, A. S. Dyke, R. M. Neal, W. R. Peltier, A data-calibrated distribution of deglacial chronologies for the North American ice complex from glaciological modeling. *Earth Planet. Sci. Lett.* **315**, 30–40 (2012).

Crossref | Google Scholar

51 A. S. Dyke, "An outline of North American deglaciation with emphasis on central and northern Canada" in *Quaternary Glaciations—Extent and Chronology Part II: North America*, J. Ehlers, P. L. Gibbard, Eds. (Elsevier, Amsterdam, 2004), pp. 373–424.

Crossref | Google Scholar

52 D. H. Shugar et al., Post-glacial sea-level change along the Pacific coast of North America. *Quat. Sci. Rev.* **97**, 170–192 (2014).

Crossref | Google Scholar

53 C. M. Darvill, B. Menounos, B. M. Goehring, O. B. Lian, M. W. Caffee, Retreat of the western Cordilleran Ice Sheet margin during the last deglaciation. *Geophys. Res. Lett.* **45**, 9710–9720 (2018).

Crossref | Google Scholar

54 A. J. Lesnek, J. P. Briner, C. Lindqvist, J. F. Baichtal, T. H. Heaton, Deglaciation of the Pacific coastal corridor directly preceded the human colonization of the Americas. *Sci. Adv.* **4**, eaar5040 (2018).

Crossref | PubMed | Google Scholar

55 A. S. Dalton et al., An updated radiocarbon-based ice margin chronology for the last deglaciation of the North American Ice Sheet Complex. *Quat. Sci. Rev.* **234**, 106223 (2020).

Crossref | Google Scholar

56 G. M. D. Hartman, J. J. Clague, Quaternary stratigraphy and glacial history of the Peace River valley, northeast British Columbia. *Can. J. Earth Sci.* **45**, 549–564 (2008).

Crossref | Google Scholar

57 J. K. Cuzzone et al., Final deglaciation of the Scandinavian Ice Sheet and implications for the Holocene global sea-level budget. *Earth Planet. Sci. Lett.* **448**, 34–41 (2016).

Crossref | Google Scholar

58 N. Lifton, T. Sato, T. J. Dunai, Scaling in situ cosmogenic nuclide production rates using analytical approximations to atmospheric cosmic-ray fluxes. *Earth Planet. Sci. Lett.* **386**, 149–160 (2014).

Crossref | Google Scholar

59 A. E. Carlson, Comment on: Deglaciation of the Greenland and Laurentide ice sheets interrupted by glacier advance during abrupt coolings. *Quat. Sci. Rev.* **240**, 106354 (2020).

Crossref | Google Scholar

Further reading in this issue

RESEARCH ARTICLE | MARCH 30, 2022 |

Carbon sources and pathways for citrate secreted by human prostate cancer cells determined by NMR tracing and metabolic modeling

Frits H. A. van Heijster, Vincent Breukels, [...] Arend Heerschap

RESEARCH ARTICLE | MARCH 28, 2022 |

Analysis of biodiversity data suggests that mammal species are hidden in predictable places

Danielle J. Parsons, Tara A. Pelletier, [...] Bryan C. Carstens

RESEARCH ARTICLE | MARCH 28, 2022 |

Solid organic-coated ammonium sulfate particles at high relative humidity in the summertime Arctic atmosphere

Rachel M. Kirpes, Ziying Lei, [...] Andrew P. Ault

Trending

RESEARCH ARTICLE | JUNE 25, 2025 |

Generative AI without guardrails can harm learning: Evidence from high school mathematics

While generative AI has been shown to enhance productivity, its influence on learning new skills remains unclear. Our…

Hamsa Bastani, Osbert Bastani, […] Rei Mariman

RESEARCH ARTICLE | MAY 19, 2026 |

Large language models pass a standard three-party Turing test

The Turing test asks whether a machine can imitate human behavior so well that another human cannot reliably tell the…

Cameron R. Jones and Benjamin K. Bergen

OPINION | MAY 27, 2026 |

Ecology is not yet ready for AI—and why that matters

Gayatri Mishra